

Pathways for the $\text{OH} + \text{Cl}_2 \rightarrow \text{HOCl} + \text{Cl}$ and $\text{HOCl} + \text{Cl} \rightarrow \text{HCl} + \text{ClO}$ Reactions

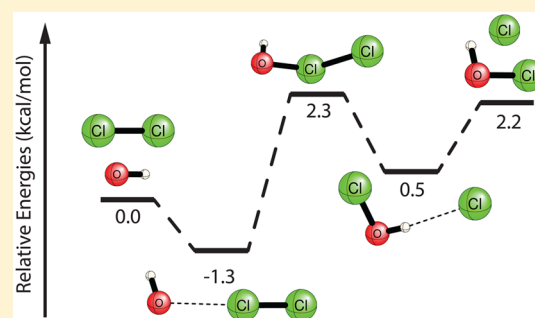
Hongyan Wang,^{*,†,‡} Yudong Qiu,[‡] Gábor Czakó,[§] and Henry F. Schaefer III[‡]

[†]School of Physical Science and Technology, Southwest Jiaotong University, Key Laboratory of Advanced Technologies of Materials, Ministry of Education of China, Chengdu 610031, China

[‡]Department of Chemistry and Center for Computational Quantum Chemistry, University of Georgia, Athens, Georgia 30602, United States

[§]Laboratory of Molecular Structure and Dynamics, Institute of Chemistry, Eötvös University, P.O. Box 32, H-1518 Budapest 112, Hungary

ABSTRACT: High level coupled-cluster theory, with spin–orbit coupling evaluated via the Breit–Pauli operator in the interacting-states approach, is used to investigate the OH radical reaction with Cl_2 and the subsequent reaction $\text{HOCl} + \text{Cl}$. The entrance complex, transition state, and exit complex for both reactions have been determined using the CCSD(T) method with correlation consistent basis sets up to cc-pV6Z. Also reported are CCSDT computations. The $\text{OH} + \text{Cl}_2$ reaction is predicted to be endothermic by 2.2 kcal/mol, compared to the best experiments, 2.0 kcal/mol. The above theoretical results include zero-point vibrational energy corrections and spin–orbit contributions. The activation energy (E_a) of the $\text{OH} + \text{Cl}_2$ reaction predicted here, 2.3 kcal/mol, could be as much as 1 kcal/mol too high, but it falls among the four experimental E_a values, which span the range 1.1–2.5 kcal/mol. The exothermicity of the second reaction $\text{HOCl} + \text{Cl} \rightarrow \text{HCl} + \text{ClO}$ is 8.4 kcal/mol, compared to experiment 8.7 kcal/mol. The activation energy for latter reaction is unknown experimentally, but predicted here to be large, 11.5 kcal/mol. There are currently no experiments relevant to the theoretical entrance and exit complexes predicted here.



1. INTRODUCTION

With the manufacture of chlorine-containing compounds, such as ethylene dichloride and chlorinated solvents, chlorine as a waste gas enters the atmosphere in large quantities. The chemistry of the chlorine oxides, including ClO, play an important role in atmospheric chemistry.¹ At the same time, the OH radical plays a widely recognized important role in both atmospheric and combustion chemistry,² and its interactions with chlorine are important. In this context, the $\text{OH} + \text{Cl}_2 \rightarrow$ products reaction has been the subject of both experimental and theoretical studies.

In 1979, Leu and Lin performed perhaps the first modern experimental investigation of the $\text{OH} + \text{Cl}_2$ reaction, using a discharge flow system at 298 K and determining the rate constants using resonance fluorescence detection of hydroxyl radicals.³ Rate coefficients and products have been reported experimentally by Ravishankara, Eisele, and Wine,⁴ by Loewenstein and Anderson,^{5,6} and by Boudaghians, Hall, and Wayne.⁷ However, the reported experimental rate coefficients and activation energies have notable uncertainties (see Grills, Burkholder, and Ravishankara⁸). Consequently, theoretical investigations of the reaction have been carried out. Kosmas and Drougas⁹ and Melissas and co-workers¹⁰ investigated the dynamics of the $\text{OH} + \text{Cl}_2 \rightarrow \text{HOCl} + \text{Cl}$ reaction via quasiclassical dynamical calculations on different potential

energy surfaces, some constructed from unrestricted second-order Møller–Plesset perturbation theory. The temperature dependence of the rate coefficients for the $\text{OH} + \text{Cl}_2 \rightarrow \text{HOCl} + \text{Cl}$ reaction has been derived from experimental data, modeling, and thermochemical information by Dellinger and co-workers.¹¹ Their reaction energies for different $\text{OH} + \text{Cl}_2 \rightarrow \text{HOCl} + \text{Cl}$ pathways were obtained from density functional theory and the QCISD method.

As a classic example of the role of the intact OH bond in the dynamics of a diatom–diatom reaction, an accurate theoretical assessment of these processes should be helpful for understanding reaction mechanisms and strategies to predict and control increased halogen and interhalogen exhaust emissions.

Recently, a surprising quenching of the spin–orbit interaction was found to significantly diminish the dissociation energies of the $\text{H}_2\text{O}\cdots\text{X}$ [$\text{X} = \text{F}, \text{Cl}, \text{Br}, \text{I}$] systems.¹² In this context, the $\text{Cl}\cdots\text{HOCl}$ complex, accessible during the $\text{OH} + \text{Cl}_2$ reaction, may be

Special Issue: 100 Years of Combustion Kinetics at Argonne: A Festschrift for Lawrence B. Harding, Joe V. Michael, and Albert F. Wagner

Received: February 6, 2015

Revised: May 4, 2015

Published: May 12, 2015

similar to that for the $\text{Cl}\cdots\text{H}_2\text{O}$ entrance complex, where an 87% quenching of the spin–orbit correction was found. In the present research, spin–orbit considerations should provide more reliable reaction energies and the detailed reaction mechanisms for the reactions $\text{OH} + \text{Cl}_2$ and $\text{HOCl} + \text{Cl}$. Highly accurate theoretical results with spin–orbit coupling corrections may assist in identifying the dynamics characterizing the other halogen and interhalogen reactions $\text{OH} + \text{XX}'$ ($X, X' = \text{F}, \text{Br}, \text{I}$).

2. METHODOLOGY

Critical features of the potential energy surface for the $\text{OH} + \text{Cl}_2$ reaction have been studied here using high level theoretical methods, i.e., the coupled-cluster single and double substitution method with perturbative treatment of triple excitations CCSD(T) .^{13–15} Spin-restricted treatments are employed for both the Hartree–Fock and coupled cluster wave functions. The correlation-consistent polarized valence basis sets of Dunning, Kendall, Harrison, Woon, and Peterson, including cc-pVDZ, cc-pVTZ, cc-pVQZ, and cc-pVSZ are employed to optimize the structures of the reactants, entrance complex, transition states, exit complex, and the products.^{16–19} The stationary points are characterized by harmonic vibrational frequency analyses with the $\text{CCSD(T)}/\text{cc-pVQZ}$ method. Single-point energies were evaluated with the $\text{CCSD(T)}/\text{cc-pV6Z}$ method. Additional CCSDT (cc-pVTZ basis) computations are reported. Subsequently, the intrinsic reaction coordinate (IRC)^{20,21} method in Gaussian 09²² is used with the M05/DZP DFT method²³ to confirm that the transition states connect the designated entrance and exit complexes, where the DZP basis sets are the Huzinaga–Dunning double- ζ plus polarization Gaussian sets.^{24,25}

The spin–orbit (SO) computations employ the Breit–Pauli operator in the interacting-states approach.²⁶ This method requires multireference *ab initio* computations^{27,28} to obtain the eigenfunctions of the non-SO electronic Hamiltonian. Subsequently, the SO eigenstates are obtained by diagonalizing the SO Hamiltonian in the basis of the non-SO wave functions. In the present study the three lowest-energy non-SO doublet states are computed for Cl and $\text{Cl}\cdots\text{HOCl}$, whereas four doublet states are chosen for the other stationary points. The SO eigenstates are obtained by diagonalizing 6×6 (Cl and $\text{Cl}\cdots\text{HOCl}$) and 8×8 (other stationary points) SO matrices.

The SO energy computations are based on the $\text{CCSD(T)}/\text{cc-pVQZ}$ optimized geometries. The electronic states of the non-SO Hamiltonian are obtained by different multireference methods. First, multiconfigurational self-consistent field (MCSCF) computations are performed using the cc-pVDZ and cc-pVTZ basis sets. Second, a Davidson-corrected²⁹ multireference configuration interaction (MRCI+Q) approach is employed with the cc-pVDZ basis to account for dynamical correlation effects on the SO corrections. All the MCSCF and MRCI+Q computations utilize the full-valence active space, i.e., 21 electrons in 13 spatial orbitals (21e, 13o) for the entrance and exit complexes and transition states, (7e, 5o) for OH, (7e, 4o) for the Cl atom, and (13e, 8o) for ClO. For the MRCI+Q computations the usual frozen-core approach is employed.

All CCSD(T) and SO computations are performed using the MOLPRO package.³⁰ The MRCC program of Kállay³¹ interfaced to MOLPRO was used to obtain the CCSDT energies.

3. RESULTS AND DISCUSSIONS

3.1. Stationary Point Geometries. The two reactions investigated here are



The reactants, entrance complexes, transition states, exit complexes, and products are optimized with the CCSD(T) method (Figures 1 and 2). The optimized energies E (hartree)

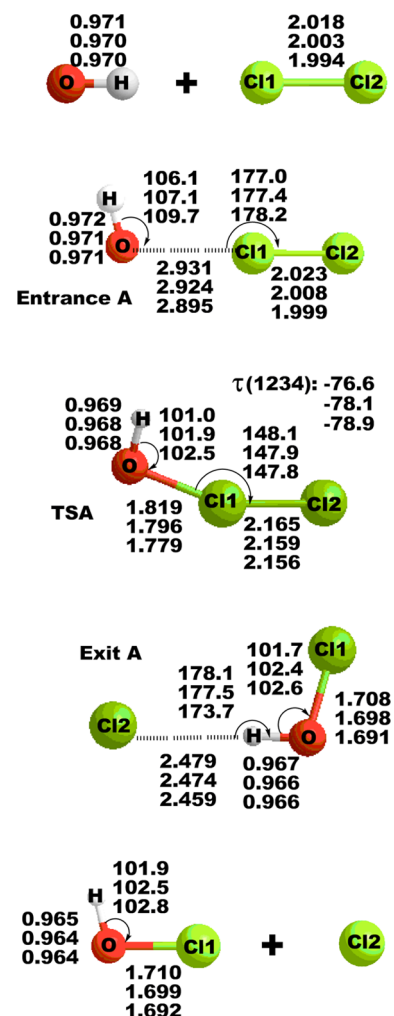


Figure 1. Optimized geometries of the reactants, entrance complex, transition state, exit complex, and products for reaction A, namely $\text{OH} + \text{Cl}_2$. The distances (Å) from top to bottom are from the cc-pVTZ, cc-pVQZ, and cc-pVSZ basis sets, respectively, with the CCSD(T) method. For the transition state structure, $\tau(1234)$ is the dihedral angle.

and harmonic vibrational frequencies ω (cm^{-1}) for all the stationary points are shown in Tables 1 and 2. Consider first reaction A. When the OH radical approaches Cl_2 , there is an entrance complex $\text{H–O}\cdots\text{Cl–Cl}$ in the reactant valley. The resulting equilibrium $\text{O}\cdots\text{Cl}$ distance is 2.895 Å with the $\text{CCSD(T)}/\text{cc-pVSZ}$ method. Although the H–O and Cl–Cl moieties lie in the same plane, the four-atom system is not collinear. The $\text{O}\cdots\text{Cl}$ linkage twists out of the plane to dihedral angle 79° when the first transition state (TSA) is formed, with an imaginary vibrational frequency of $737i$ cm^{-1} (cc-pVTZ) and $559i$ cm^{-1} (cc-pVQZ). The significant variation as a function of

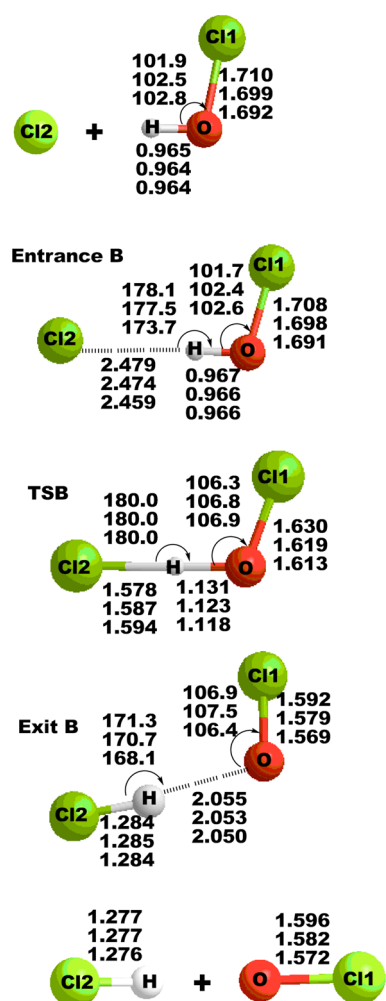


Figure 2. Optimized geometries of the reactants, entrance complex, transition state, exit complex, and products for reaction B, namely HOCl + Cl. The distances (Å) from top to bottom are from the cc-pVTZ, cc-pVQZ, and cc-pVSZ basis sets, respectively, with the CCSD(T) method.

basis set is a bit surprising. The corresponding twist normal mode leads to the exit complex A, namely Cl \cdots H–O–Cl, in the product valley, for which Cl \cdots H–O is almost collinear. From exit complex

A, the Cl \cdots H connection with distance 2.459 Å (cc-pVSZ) breaks to yield the separated products HOCl and Cl.

Now consider reaction B, namely HOCl + Cl. Entrance complex B, namely Cl \cdots H–O–Cl, exists in the reactant valley. Following the Cl \cdots H vibrational coordinate, one finds the transition state TSB, which has a large imaginary vibrational frequency of 1530i cm⁻¹ (cc-pVTZ) or 1328i cm⁻¹ (cc-pVQZ). The imaginary TSB normal mode leads to exit complex B, namely Cl–H \cdots O–Cl, after which the H \cdots O bond is broken, leading to products HCl and ClO.

On the HOClCl potential energy surface, we find a total of three complexes and two transition states (TSA, TSB) predicted by the CCSD(T) method, roughly similar to the density functional method BH&HLYP/aug-cc-pVDZ optimization results of Bryukov and co-workers.¹¹ However, the exit complex A predicted here by the CCSD(T) method is intermediate between the TSA and TSB structures predicted by the BH&HLYP/aug-cc-pVDZ DFT method.¹⁰ No other intermediate product is found in the reactant valley for the reaction HOCl + Cl. We note that the loosely bound Cl \cdots H–O–Cl structure is both the exit complex for reaction A and the entrance complex for reaction B.

3.2. Energetics. i. Classical Energetics. Relative energies without zero-point vibrational energy or spin-orbit corrections (this is what we mean by the word “classical”) for all stationary points of both reactions are reported in Figures 3 (reaction A) and 4 (reaction B). Reaction A is predicted to be exothermic by 1.3 and 0.3 kcal/mol with the cc-pVTZ and cc-pVQZ basis sets, respectively, without ZPVE corrections. However, with the larger basis sets, cc-pVSZ and cc-pV6Z, reaction A is endothermic by 0.4 and 0.6 kcal/mol, respectively. The latter endothermicity is changed by only +0.05 kcal/mol with the full CCSDT method. The CCSD(T) classical reaction barrier height is 3.8, 2.2, 1.5, and 1.2 kcal/mol, respectively, with the TZ, QZ, 5Z, and 6Z basis sets. This CCSD(T) barrier height is seen to be quite sensitive to the basis set. The full CCSDT correction reduces the classical barrier by a rather large 1.36 kcal/mol. The entrance complex A, H–O \cdots Cl–Cl, is predicted to lie 1.9 kcal/mol below the separated reactants OH + Cl₂. Exit complex A, Cl \cdots H–O–Cl, is predicted to lie 2.0 kcal/mol below the separated products HOCl + Cl, and 1.5 kcal/mol below the separated reactants OH + Cl₂.

The exothermicity for reaction B, HOCl + Cl \rightarrow HCl + ClO, is 2.7, 3.9, 4.8, or 5.1 kcal/mol, respectively, predicted with the cc-

Table 1. Energies (E , hartrees) and Harmonic Vibrational Frequencies (ω , cm⁻¹) for the Stationary Points for Reaction A: OH + Cl₂ \rightarrow HOCl + Cl^a

		cc-pVTZ	cc-pVQZ	cc-pVSZ	cc-pV6Z
OH	E	-75.63756	-75.66144	-75.66941	-75.67201
	ω	3745	3750		
Cl ₂	E	-919.42662	-919.47571	-919.49246	-919.50007
	ω	542	551		
entrance A	E	-995.06751	-995.14025	-995.16489	-995.17515
	ω	53, 57, 89, 181, 535, 3740	56, 60, 85, 189, 544, 3738		
TSA	E	-995.05814	-995.13362,	-995.15956	-995.17022
	ω	226, 348, 445, 1090, 3767, 737i	229, 354, 453, 1100, 3765, 559i		
exit A	E	-995.06918	-995.14066	-995.16443	-995.17441
	ω	36, 99, 198, 730, 1306, 3779	31, 100, 184, 738, 1300, 3766		
HOCl	E	-535.39469	-535.44455	-535.46159	-535.46828
	ω	728, 1279, 3809	736, 1275, 3805		
Cl	E	-459.67162	-459.69305	-459.69967	-459.70292

^aAll computations reported in this table were performed with the CCSD(T) method.

Table 2. Energies (E , hartrees) and Harmonic Vibrational Frequencies (ω , cm^{-1}) for the Stationary Points for Reaction B: HOCl + Cl \rightarrow HCl + ClO^a

		cc-pVTZ	cc-pVQZ	cc-pVSZ	cc-pV6Z
HOCl	E	-535.39469	-535.44455	-535.46159	-535.46828
	ω	728, 1279, 3809	736,1275,3805		
Cl	E	-459.67162	-459.69305	-459.69967	-459.70292
	ω				
entrance B	E	-995.06918	-995.14066	-995.16443	-995.17441
	ω	36, 99, 198, 730, 1306, 3779	31, 100, 184, 738, 1300, 3766		
TSB	E	-995.04029	-995.11377	-995.13838	-995.14869
	ω	113, 484, 836, 915, 1323, 1530i	108, 489, 852, 917, 1318, 1328i		
exit B	E	-995.07605	-995.14890	-995.17392	-995.18426
	ω	40, 130, 294, 388, 837, 2907	37,129,284, 379,850,2893		
ClO	E	-534.73338	-534.78162	-534.79880	-534.80551
	ω	824	838		
HCl	E	-460.33722	-460.36213	-460.37015	-460.37380
	ω	2999	2995		

^aAll computations reported in this table were performed with the CCSD(T) method.

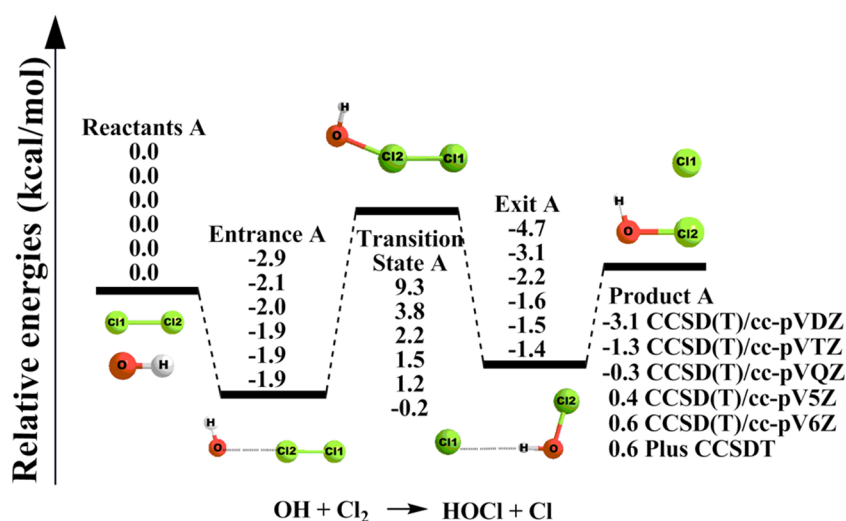


Figure 3. Stationary point classical energetics on the OH + Cl₂ reaction A potential energy surface (i.e., without ZPVE and spin-orbit corrections). The cc-pV6Z results are single-point energies, obtained by assuming the cc-pVSZ stationary geometries.

pVTZ, cc-pVQZ, cc-pVSZ, and cc-pV6Z basis sets, respectively. Full triple excitations significantly increase this exothermicity, to 6.0 kcal/mol. The reaction B CCSD(T) barrier height is 16.3, 15.0, 14.4, and 14.1 kcal/mol, respectively, with the TZ, QZ, SZ, and 6Z basis sets. Although sensitive to the basis set, the barrier is much higher than that for the above-discussed reaction A, OH + Cl₂. With the full CCSDT correction, the classical barrier is 13.8 kcal/mol. Transition state B is predicted to lie 15.8 kcal/mol higher in energy than entrance complex B, namely Cl \cdots H–O–Cl, which is also the exit complex for reaction A. Entrance complex B lies 2.0 kcal/mol below the separated reactants with 6Z basis set. Exit complex B, ClH \cdots OCl, lies 9.1 kcal/mol below the reactants HOCl + Cl and 3.1 kcal/mol below the separated products HCl + ClO.

ii. Energetics with Zero-Point Vibration. The relative energy ordering of the stationary points is not changed by the zero-point vibrational energy corrections. Considering the zero-point vibrational energy (ZPVE) corrections (Table 3), the reaction A endothermicity is 0.9, 1.9, 2.6, or 2.7 kcal/mol, respectively, with the cc-pVTZ, cc-pVQZ, cc-pVSZ, and cc-pV6Z basis sets. It is seen that the ZPVE corrections shift reaction A from 0.6 to 2.7 kcal/mol endothermic. The ZPVE corrections increase the CCSD(T) classical barrier for reaction A to 6.1, 4.5, 3.7, and 3.5

kcal/mol, respectively, for the TZ, QZ, SZ, and 6Z basis sets. The effect of ZPVE on the barrier is substantial, changing the classical barrier from 1.2 to 3.5 kcal/mol. The origin of this change lies with the facts that (a) the OH frequencies of the isolated diatomic (3750 cm^{-1}) and that of TSA (3765 cm^{-1}) are the same to within 15 cm^{-1} and (b) the frequency of isolated Cl₂ is only 551 cm^{-1} , much less than the sum of the other (than OH stretch) four real frequencies (1100, 453, 354, and 229 cm^{-1}) of the transition state.

For reaction B, the ZPVE-corrected exothermicity is 5.5, 6.7, 7.7, or 7.9 kcal/mol predicted with the cc-pVTZ, cc-pVQZ, cc-pVSZ, and cc-pV6Z basis sets, respectively (Table 4). Again, the ZPVE correction is substantial, namely, 7.9 – 5.1 = 2.8 kcal/mol. This change is due to the departure of the large OH stretching frequency (for HOCl 3805 cm^{-1}) from the products HCl + ClO. The reaction B ZPVE-corrected barrier height is 13.3, 11.9, 11.3, or 11.1 kcal/mol, respectively, with our four correlation consistent basis sets. For this barrier, the ZPVE reduces the magnitude by 14.1 – 11.1 = 3.0 kcal/mol. Due to the absence of anharmonicity in our zero-point computations, the ZPVE corrections are perhaps as much as 10% too big. Even so, these zero-point corrections to the energetics are large.

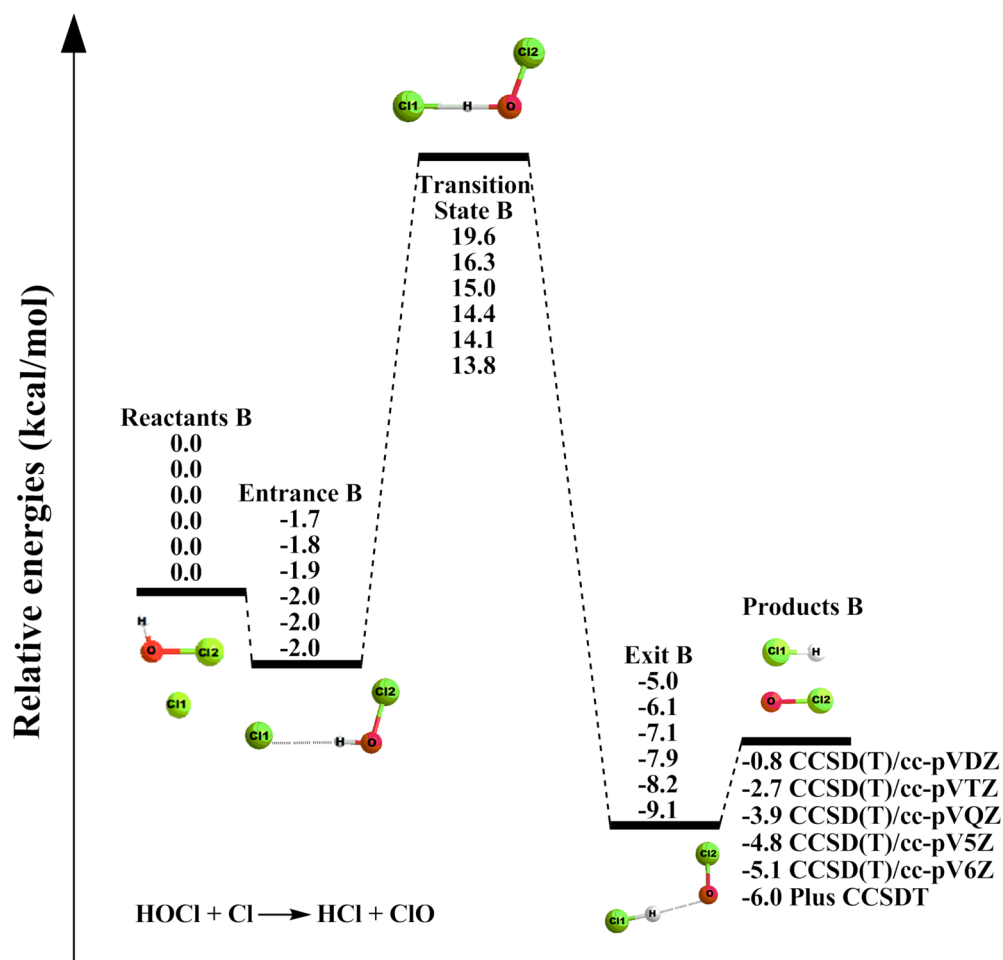


Figure 4. Stationary point classical energetics on the HOCl + Cl reaction B potential energy surface (i.e., without ZPVE and spin-orbit corrections). The cc-pV6Z results are single-point energies, obtained by assuming the cc-pV5Z stationary geometries.

Table 3. Energies (E , kcal/mol) Relative to OH + Cl₂ and Zero-Point Vibrational Energy Corrected Energies ($E+ZPVE$, kcal/mol) for the Stationary Points of Reaction A: OH + Cl₂ \rightarrow HOCl + Cl

	cc-pVTZ		cc-pVQZ		cc-pV5Z		cc-pV6Z	
	E	$E+ZPVE$	E	$E+ZPVE$	E	$E+ZPVE$	E	$E+ZPVE$
OH + Cl ₂	0.00	0.00	0.00	0.00	0.00	0.00	0.00	0.00
entrance A	-2.09	-1.57	-1.95	-1.42	-1.90	-1.37	-1.93	-1.40
TSA	3.79	6.06	2.22	4.50	1.45	3.74	1.17	3.46
exit A	-3.13	-0.52	-2.21	0.35	-1.61	0.94	-1.46	1.10
HOCl + Cl	-1.33	0.85	-0.28	1.88	0.38	2.55	0.55	2.72

Table 4. Energies (E , kcal/mol) Relative to HOCl + Cl and Zero-Point Vibrational Energy Corrected Energies ($E+ZPVE$, kcal/mol) for the Stationary Points of Reaction B: HOCl + Cl \rightarrow HCl + ClO

	cc-pVTZ		cc-pVQZ		cc-pV5Z		cc-pV6Z	
	E	$E+ZPVE$	E	$E+ZPVE$	E	$E+ZPVE$	E	$E+ZPVE$
HOCl + Cl	0.00	0.00	0.00	0.00	0.00	0.00	0.00	0.00
entrance B	-1.80	-1.38	-1.92	-1.53	-1.99	-1.60	-2.01	-1.62
TSB	16.32	13.25	14.95	11.90	14.36	11.31	14.12	11.07
exit B	-6.12	-7.92	-7.09	-8.92	-7.94	-9.77	-8.20	-10.03
HCl + ClO	-2.69	-5.54	-3.86	-6.70	-4.82	-7.66	-5.09	-7.93

iii. Spin-Orbit Effects. Our spin-orbit predictions are summarized in Tables 5 and 6. The SO corrections are defined as the difference between the SO and non-SO ground state electronic energies, i.e., $\Delta_{SO} = E_{SO}(\text{ground state}) - E_{\text{non-SO}}(\text{ground})$. The cc-pVDZ and cc-pVTZ MCSCF results

agree to within 0.04 kcal/mol, whereas the MCSCF/cc-pVDZ and MRCI+Q/cc-pVDZ levels give the same SO corrections to within 0.03 kcal/mol. Thus, it appears that the present SO corrections are satisfactorily converged with respect to the basis size and the treatment of electron correlation. The theoretical SO

Table 5. Spin–Orbit Corrections (kcal/mol) at Different Levels of Theory for the Stationary Points of Reaction A: OH + Cl₂ → HOCl + Cl^a

	MCSCF/cc-pVDZ		MCSCF/cc-pVTZ		MRCI+Q/cc-pVDZ	
	Δ_{SO}	Δ_{SO}^*	Δ_{SO}	Δ_{SO}^*	Δ_{SO}	Δ_{SO}^*
OH + Cl ₂	-0.19	0.00	-0.20	0.00	-0.18	0.00
entrance A	-0.05	+0.14	-0.05	+0.15	-0.02	+0.16
TSA	-0.01	+0.17	-0.01	+0.18	-0.01	+0.17
exit A	-0.76	-0.58	-0.76	-0.56	-0.79	-0.61
HOCl + Cl	-0.78	-0.59	-0.78	-0.59	-0.75	-0.57

^a Δ_{SO}^* is the SO correction relative to that for separated OH + Cl₂.

Table 6. Spin–Orbit Corrections (kcal/mol) at Different Levels of Theory for the Stationary Points of Reaction B: HOCl + Cl → HCl + ClO^a

	MCSCF/cc-pVDZ		MCSCF/cc-pVTZ		MRCI+Q/cc-pVDZ	
	Δ_{SO}	Δ_{SO}^*	Δ_{SO}	Δ_{SO}^*	Δ_{SO}	Δ_{SO}^*
HOCl + Cl	-0.78	0.00	-0.78	0.00	-0.75	0.00
entrance B	-0.76	+0.02	-0.76	+0.02	-0.79	-0.04
TSB	-0.06	+0.72	-0.06	+0.72	-0.07	+0.68
exit B	-0.06	+0.72	-0.07	+0.71	-0.06	+0.69
HCl + ClO	-0.34	+0.44	-0.38	+0.41	-0.36	+0.39

^a Δ_{SO}^* is the SO correction relative to that for separated HOCl + Cl.

corrections lower the OH + Cl₂, Cl + HOCl, and HCl + ClO asymptotes by 0.20, 0.78, and 0.38 kcal/mol, respectively. These MCSCF/cc-pVTZ SO corrections agree reasonably with the corresponding experimental SO values [0.20 (OH), 0.84 (Cl), and 0.45 (ClO) kcal/mol].³² The latter results are obtained from the measured SO splittings of OH ($\epsilon = 0.40$), Cl ($\epsilon = 2.52$), and ClO ($\epsilon = 0.91$) (ϵ in kcal/mol) as $\epsilon/2$, $\epsilon/3$, and $\epsilon/2$, respectively.

In reaction A, the SO correction of the entrance complex HO...ClCl is significantly quenched to -0.05 kcal/mol with the MCSCF/cc-pVTZ method. The MRCI+Q/cc-pVDZ method gives a slightly larger quenching, as the MRCI+Q SO correction for the entrance complex HO...ClCl is only -0.02 kcal/mol. At the transition state TSA itself, the SO correction is small, i.e., -0.01 kcal/mol. The TSA barrier height and the relative energy of the HO...ClCl entrance complex thus increase by about 0.18 and 0.15 kcal/mol, respectively, because the SO correction lowers the reactant asymptote and has little effect on the energies of the above two stationary points. Perhaps surprisingly, the SO correction for the exit Cl...HOCl complex (-0.76 kcal/mol), with its 2.47 Å Cl...H equilibrium distance, is almost the same as that of the Cl atom (-0.78 kcal/mol). This can be contrasted with the Cl...H₂O complex, where 87% quenching of the SO correction was found recently.¹² An explanation is allowed by the fact that Cl...HOCl is a H-bonded complex, whereas Cl binds to the O atom in Cl...H₂O (the O...Cl separation is 2.59 Å). For Cl...HOCl we have investigated the Cl...H distance dependence of the SO correction at the MCSCF/cc-pVDZ level and find that the quenchings are 3%, 62%, and 98% at Cl...H internuclear separations 2.0, 1.6, and 1.2 Å, respectively. It is important to note that the quantity $E_{\text{SO}}(\text{ground state}) - E_{\text{non-SO}}(\text{ground state})$ is almost constant at Cl...H distances larger than 2.0 Å.

Now consider the SO effects on reaction B, HOCl + Cl → HCl + ClO. The SO corrections for the transition state TSB and the exit complex B, ClH...OCl, are both small, i.e., -0.06 and -0.07 kcal/mol. In contrast, the energies of both HOCl + Cl and Cl...

H-O-Cl decrease by 0.8 kcal/mol; thus, the SO effect on the energy of Cl...H-O-Cl is negligible relative to the reactants HOCl + Cl. The energies of both TSB and exit complex B, ClH...OCl, increase by 0.7 kcal/mol relative to reactants HOCl + Cl, because the SO interaction lowers the reactant asymptote and has little effect on the TSB and ClH...OCl energies. Finally, the relative energy of the HCl + ClO product channel increases by about 0.4 kcal/mol, because the SO splitting of Cl is larger than that for ClO.

iv. Comparison with Experiment. Our predicted energetics are summarized in Tables 7 and 8. For reaction A, the

Table 7. Final Theoretical Predictions for the Energetics (kcal/mol) of Reaction A: OH + Cl₂ → HOCl + Cl^a

	classical	zero-point vibration corrected	spin-orbit correction	final predictions
OH + Cl ₂	0.00	0.00	0.00	0.00
entrance A	-1.94	-1.41	+0.16	-1.25
TSA	-0.19	2.10	+0.17	2.27
exit A	-1.41	1.15	-0.61	0.54
HOCl + Cl	0.60	2.77	-0.57	2.20

^aThe "Classical" energetics are the CCSD(T)/cc-pV6Z relative energies corrected by the full CCSDT increments obtained with the cc-pVTZ basis set.

Table 8. Final Theoretical Predictions for the Energetics (kcal/mol) of Reaction B: HOCl + Cl → HCl + ClO^a

	classical	zero-point vibration corrected	spin-orbit correction	final predictions
HOCl + Cl	0.00	0.00	0.00	0.00
entrance B	-2.01	-1.62	-0.04	-1.66
TSB	13.82	10.77	+0.68	11.45
exit B	-9.12	-10.95	+0.69	-10.26
HCl + ClO	-5.96	-8.80	+0.39	-8.41

^aThe "Classical" energetics are the CCSD(T)/cc-pV6Z relative energies corrected by the full CCSDT increments obtained with the cc-pVTZ basis set.

exothermicity and barrier height may be compared to experimental values. Due to prior uncertainties in heats of formation of HOCl and Cl, the experimental values of the reaction A exothermicity vary somewhat. Lowenstein and Anderson⁵ report $\Delta H = +1.8$ kcal/mol. Wayne and co-workers⁷ conclude 1.0 kcal/mol. Ravishankara and co-workers⁴ find 1.6 kcal/mol but suggest an uncertainty of 3 kcal/mol for the heat of formation of HOCl. Finally, Dellinger and co-workers¹¹ favor 2.3 ± 0.8 kcal/mol. The Active Thermochemical Tables of Ruscic and co-workers³³ provide the most reliable energetics for reaction A. For this purpose we use Ruscic's 0 K heats of formation for OH (37.25 kJ/mol), Cl (119.62 kJ/mol), and HOCl (-73.87 kJ/mol). In this way the OH + Cl₂ → HOCl + Cl reaction is found to be endothermic by 2.0 kcal/mol, in good agreement with the four earlier experimental values. Our final prediction (Table 7) of 2.2 kcal/mol is in close agreement with the endothermicity derived from the Active Thermochemical Tables.^{33–35}

For the OH + Cl₂ reaction A, we find four experimental activation energies in the literature, namely 2.1 kcal/mol (Anderson⁵), 1.8 ± 0.7 kcal/mol (Wayne⁷), 2.5 kcal/mol (Ravishankara⁴), and 2.3 kcal/mol (Dellinger¹¹). All of these experimental values are compatible with the present theoretical prediction of 2.3 kcal/mol.

The reaction energy for $\text{HOCl} + \text{Cl} \rightarrow \text{HCl} + \text{ClO}$ reaction B should be known experimentally. From Ruscic's Active Thermochemical Tables,³³ the 0 K heats of formation are 119.62 (Cl), -73.87 (HOCl), -92.13 (HCl), and 101.12 (ClO) kJ/mol. The experimental exothermicity for $\text{HOCl} + \text{Cl} \rightarrow \text{HCl} + \text{ClO}$ is thus 8.7 kcal/mol, in satisfactory agreement with theory, 8.4 kcal/mol.

4. CONCLUSIONS

Including the spin-orbit correction and zero-point vibrational energies corrections, the relative energies of the reactants, entrance complex, transition state, exit complex, and products for reaction A are 0.0, -1.3, +2.3, +0.5, and +2.2 kcal/mol at the CCSD(T)/cc-pV6Z level with CCSDT increments, respectively. Agreement with experiment is excellent for both the endothermicity and activation energy. The reaction B stationary point energies relative to reactants $\text{HOCl} + \text{Cl}$, at the CCSD(T)/cc-pV6Z level with CCSDT increments, are 0.0 (HOCl + Cl), -1.7 (entrance B), +11.5 (TSB), -10.3 (exit B), and -8.4 (HCl + ClO) kcal/mol, respectively. The exothermicity of reaction B is in satisfactory agreement with experiment, -8.7 kcal/mol. There are no experimental energetics for the entrance and exit minima for either reaction.

The zero-point vibrational energy and spin-orbit corrections significantly influence the reaction energy for $\text{OH} + \text{Cl}_2 \rightarrow \text{HOCl} + \text{Cl}$, due to its small endothermicity. In particular, the spin-orbit interaction influence on the reaction energy for $\text{OH} + \text{Cl}_2 \rightarrow \text{HOCl} + \text{Cl}$ is much greater than that for reaction B. We see that highly reliable theoretical methods can assist experimental analyses and be used to treat other reactions not readily studied in the laboratory.

AUTHOR INFORMATION

Corresponding Author

*H. Wang. E-mail: ccq@uga.edu.

Notes

The authors declare no competing financial interest.

ACKNOWLEDGMENTS

H.Y.W. is grateful for financial support from the China Scholarship Council, the China National Science Foundation (Grants 11174237 and 11404268), the Sichuan Province Applied Science and Technology Project (Grant 2013JY0035), and the Fundamental Research Funds for the Central Universities (2682014ZT30). G.C. thanks the Scientific Research Fund of Hungary (OTKA, NK-83583 and PD-111900) and the János Bolyai Research Scholarship of the Hungarian Academy of Sciences for financial support. Y.Q. and H.F.S. are supported by the U.S. Department of Energy, Office of Basic Energy Sciences, Chemical Sciences Division, Gas Phase Chemical Physics Program and Combustion Research. We are grateful to Dr. Branko Ruscic for sharing his Active Thermochemical Table results with us.

REFERENCES

- (1) Holloway, A. M.; Wayne, R. P. *Atmospheric Chemistry*; Royal Society of Chemistry: London, 2010.
- (2) Patra, P. K.; Kro, M. C.; Montzka, S. A.; Arnold, T.; Atlas, E. L.; Lintner, B. R.; Stephens, B. B.; et al. Observational evidence for interhemispheric hydroxyl-radical parity. *Nature* **2014**, *513*, 219–223.
- (3) Leu, M. T.; Lin, C. L. Rate constants for the reactions of hydroxyl with chlorine monoxide, chlorine, and dichlorine monoxide at 298 K. *Geophys. Res. Lett.* **1979**, *6*, 425–428.

- (4) Ravishankara, A. R.; Eisele, F. L.; Wine, P. H. The kinetics of the reaction of hydroxyl radical with chlorine monoxide. *J. Chem. Phys.* **1983**, *78*, 1140–1144.

- (5) Loewenstein, L. M.; Anderson, J. G. Rate and product measurements for the reactions of hydroxyl with molecular chlorine, molecular bromine, and bromine chloride (BrCl) at 298 K. Trend interpretations. *J. Phys. Chem.* **1984**, *88*, 6277–6286.

- (6) Loewenstein, L. M.; Anderson, J. G. Rate and product measurements for the reactions of hydroxyl with molecular iodine and iodine chloride at 298 K: separation of gas-phase and surface reaction components. *J. Phys. Chem.* **1985**, *89*, 5371–5379.

- (7) Boudaghians, R. B.; Hall, I. W.; Wayne, R. P. Kinetics of the reactions of the hydroxyl radical with molecular chlorine and bromine. *J. Chem. Soc., Faraday Trans.2* **1987**, *83*, 529–538.

- (8) Gilles, M. K.; Burkholder, J. B.; Ravishankara, A. R. Rate coefficients for the reaction of OH with Cl_2 , Br_2 , and I_2 from 235 to 354 K. *Int. J. Chem. Kinet.* **1999**, *31*, 417–424.

- (9) Kosmas, A. M.; Drougas, E. Quasiclassical trajectory calculations of the diatom-diatom reaction $\text{OH} + \text{Cl}_2 \rightarrow \text{HOCl} + \text{Cl}$ using two model potential energy surfaces. *Chem. Phys.* **1997**, *229*, 233–244.

- (10) Melissas, V. S.; Drougas, E.; Bakalbassis, E. G.; Kosmas, A. M. Dynamics of the $\text{OH} + \text{Cl}_2 \rightarrow \text{HOCl} + \text{Cl}$ reaction: Ab initio investigation and quasiclassical trajectory calculations of reaction selectivity. *J. Phys. Chem. A* **2000**, *104*, 626–634.

- (11) Bryukov, M. G.; Knyazev, V. D.; Lomnicki, S. M.; McFerrin, C. A.; Dellinger, B. Temperature-dependent kinetics of the gas-phase reactions of OH with Cl_2 , CH_4 , and C_3H_8 . *J. Phys. Chem. A* **2004**, *108*, 10464–10472.

- (12) Czakó, G.; Császár, A. G.; Schaefer, H. F. Surprising quenching of the spin-orbit interaction significantly diminishes $\text{H}_2\text{O}\cdots\text{X}$ [$\text{X} = \text{F}, \text{Cl}, \text{Br}, \text{I}$] dissociation energies. *J. Phys. Chem. A* **2014**, *118*, 11956–11961.

- (13) Purvis, G. D.; Bartlett, R. J. A full coupled-cluster singles and doubles model: the inclusion of disconnected triples. *J. Chem. Phys.* **1982**, *76*, 1910–1918.

- (14) Scuseria, G. E.; Janssen, C. L.; Schaefer, H. F. An efficient reformulation of the closed-shell coupled cluster single and double excitation (CCSD) equations. *J. Chem. Phys.* **1988**, *89*, 7382–7387.

- (15) Raghavachari, K.; Trucks, G. W.; Pople, J. A.; Head-Gordon, M. A fifth-order perturbation comparison of electron correlation theories. *Chem. Phys. Lett.* **1989**, *157*, 479–483.

- (16) Dunning, T. H. Gaussian basis sets for use in correlated molecular calculations. I. The atoms boron through neon and hydrogen. *J. Chem. Phys.* **1989**, *90*, 1007–1023.

- (17) Kendall, R. A.; Dunning, T. H.; Harrison, R. J. Electron affinities of the first-row atoms revisited. Systematic basis sets and wave functions. *J. Chem. Phys.* **1992**, *96*, 6796–6806.

- (18) Woon, D. E.; Dunning, T. H. Gaussian basis sets for use in correlated molecular calculations. III. The atoms aluminum through argon. *J. Chem. Phys.* **1993**, *98*, 1358–1371.

- (19) Peterson, K. A.; Woon, D. E.; Dunning, T. H. Benchmark calculations with correlated molecular wave functions. IV. The classical barrier height of the $\text{H} + \text{H}_2 \rightarrow \text{H}_2 + \text{H}$ reaction. *J. Chem. Phys.* **1994**, *100*, 7410–7415.

- (20) Gonzalez, C.; Schlegel, H. B. An improved algorithm for reaction path following. *J. Chem. Phys.* **1989**, *90*, 2154–2161.

- (21) Gonzalez, C.; Schlegel, H. B. Reaction path following in mass-weighted internal coordinates. *J. Phys. Chem.* **1990**, *94*, 5523–5527.

- (22) Frisch, M. J.; et al. *Gaussian 09*, Revision B.01; Gaussian, Inc.: Wallingford, CT, 2010.

- (23) Zhao, Y.; Schultz, N. E.; Truhlar, D. G. Exchange-correlation functional with broad accuracy for metallic and nonmetallic compounds, kinetics, and noncovalent interactions. *J. Chem. Phys.* **2005**, *123*, 161103.

- (24) Huzinaga, S. Gaussian-type functions for polyatomic systems I. *J. Chem. Phys.* **1965**, *42*, 1293–1302.

- (25) Dunning, T. H. Gaussian basis functions for use in molecular calculations. I. Contraction of (9s5p) atomic basis sets for the first-row atoms. *J. Chem. Phys.* **1970**, *53*, 2823–2833.

- (26) Berning, A.; Schweizer, M.; Werner, H.-J.; Knowles, P. J.; Palmieri, P. Spin-orbit matrix elements for internally contracted multireference

configuration interaction wavefunctions. *Mol. Phys.* **2000**, *98*, 1823–1833.

(27) Werner, H.-J.; Knowles, P. J. An efficient internally contracted multiconfiguration-reference configuration interaction method. *J. Chem. Phys.* **1988**, *89*, 5803–5814.

(28) Knowles, P. J.; Werner, H.-J. An efficient method for the evaluation of coupling coefficients in configuration interaction calculations. *Chem. Phys. Lett.* **1988**, *145*, 514–522.

(29) Langhoff, S. R.; Davidson, E. R. Configuration interaction calculations on the nitrogen molecule. *Int. J. Quantum Chem.* **1974**, *8*, 61–72.

(30) Werner, H.-J.; Knowles, P. J.; Knizia, G.; Manby, F. R.; Schütz, M.; et al. *Molpro*, version 2012.1, a package of ab initio programs; <http://www.molpro.net>.

(31) Kállay, M.; Surján, P. R. Higher excitations in coupled-cluster theory. *J. Chem. Phys.* **2001**, *115*, 2945–2954.

(32) Huber, K. P.; Herzberg, G. *Molecular Spectra and Molecular Structure. IV. Constants of Diatomic Molecules*; Van Nostrand Reinhold Co.: New York, 1979.

(33) Ruscic, B.; Pinzon, R. E.; Morton, M. L.; Laszewski, G. V.; Bitner, S. J.; Nijssure, S. G.; Amin, K. A.; Minkoff, M.; Wagner, A. F. Introduction to active thermochemical tables: Several “key” enthalpies of formation revisited. *J. Phys. Chem. A* **2004**, *108*, 9979.

(34) Stevens, W. R.; Ruscic, B.; Baer, T. Heats of formation of C_6H_5 , $C_6H_5^+$, and C_6H_5NO by threshold photoelectron photoion coincidence and active thermochemical tables analysis. *J. Phys. Chem. A* **2010**, *114*, 13134.

(35) Ruscic, B.; Feller, D.; Peterson, K. A. Active thermochemical tables: dissociation energies of several homonuclear first-row diatomics and related thermochemical values. *Theor. Chem. Acc.* **2014**, *133*, 1415.